

Michael C. Coniglio*, David J. Stensrud, and Louis J. Wicker
 NOAA/National Severe Storms Laboratory, Norman, OK

1. INTRODUCTION

The role of vertical wind shear on the strength, structure, and maintenance of quasi-two-dimensional (2D) mesoscale convective systems (MCSs) has been examined in many contexts. Much of this work focuses on the interaction of the low-level shear with the circulation induced by the cold thunderstorm outflow (see summary in Weisman and Rotunno 2004; WR hereafter). However, the relative importance of upper-level wind shear has received comparably little attention and has been considered a passive player in the overall structure and maintenance of the systems. WR present simulations of convective systems within surface-based wind shear that extends above 5 km, but suggest that deep-shear is detrimental to producing strong quasi-2D convective systems since the overall condensation, rainfall output, and surface winds are weaker in these cases. Parker and Johnson (2004a,b) present 2D and periodic three-dimensional (3D) simulations of quasi-2D convective systems in deep shear. They stress the importance of the transient pressure perturbations in the rear-to-front acceleration of the updrafts that help to promote deep convection. In 2D, the pressure perturbations eventually lead to the transition to a more upshear-tilted system, however, the leading stratiform structures are much more persistent in the periodic 3D simulations. Combined with the fact that substantial upper-level shear and relatively weak to moderate low-level shear is frequently observed in the environments of strong, linear MCSs, including ones that contain 3D structures (Evans and Doswell 2001, Coniglio et al. 2004; CSR hereafter), this suggests that the physical mechanisms related to this upper-level shear are relevant to both quasi 2D and 3D regimes of MCSs.

This study first reexamines the basic 2D role of upper-level shear on the lifting of environmental air above cold thunderstorm outflow, which is rooted in more analytical frameworks [e.g. Moncrieff (1992), Shapiro (1992), Xu and Moncrieff (1994)]. This is accomplished through numerical simulations of density currents spreading within a vertically sheared flow using a dry, neutrally-stratified, 2D version of the National Severe Storms Laboratory Collaborative Model for Multiscale Atmospheric Simulation (NCOMMAS) (Wicker and Wilhelmson 1995). A heat sink is placed in the center of a $x=240$ km by $z=16$ km domain (with $\Delta x=\Delta z=250$ m), to introduce and maintain a spreading density current. The initial ground-relative wind perpendicular to the line changes from 0 at the surface

to 12 m s^{-1} at 2.5 km and 20 m s^{-1} at 5 km, which approximates the mean/median low-level shear-vector magnitudes associated with strong, linear MCSs (CSR).

The role of upper-level shear also is presented in 3D NCOMMAS simulations of strong MCSs. The domain is 400 km square with a horizontal grid spacing of 2 km. The vertical domain is 16 km deep with a constant 250 m grid spacing in the lowest 1.25 km (and stretched above). The initial thermodynamic profile preserves the median convective available potential energy (CAPE $\sim 2800 \text{ J kg}^{-1}$), the lifting condensation level (LCL ~ 1500 m AGL), and the maximum vertical difference in equivalent potential temperature between low-mid levels ($\theta_e \sim 30$ K) from a set of 28 strong MCS proximity soundings taken in benign synoptic-scale environments (CSR).

The basic role of upper-level shear is examined by producing seven simulations, both in 2D and 3D, in which the 5-10 km shear is increased from 0 to 30 m s^{-1} in 5 m s^{-1} increments. In the 2D simulations, the lifting of environmental air is examined through calculations of maximum vertical displacements of low-level (0-2 km) air parcels. In this context, we will show that deep-layer shear can be beneficial to the lifting of environmental air and will present evidence of this benefit in fully 3D numerical simulations of MCSs.

2. 2D RESULTS

The heat sink produces density currents with surface potential temperature deficits of 6-8 K, head depths of 2-5 km, and gust front speeds of $17\text{-}21 \text{ m s}^{-1}$, which is consistent with typical MCS cold pools (CSR). This results in a steering (critical) level (environmental wind speed = cold pool speed) between 5-7 km in all of the simulations that include upper-level shear.

The vertical motion (w) along the interface is found to decrease with increasing the upper-level shear (Fig. 1). This is the result of the development of perturbation high pressure in a flow-stagnation region above the density current head region (as seen in Fig. 7 of Shapiro 1992). This high pressure suppresses the head depth of the density current and leads to less convergence of mass along the interface. However, the pertinent point is that the maximum displacement of low-level (0-2 km) parcels actually is larger with 5, 10, and 15 m s^{-1} of upper-level-shear than it is with no upper-level-shear (Fig. 2). The maximum lifting occurs somewhere between 5 and 10 m s^{-1} of upper-level shear and then decreases to a minimum at 30 m s^{-1} . Displacements are

* Corresponding author address: Michael Coniglio, NSSL, 1313 Halley Circle, Norman, OK, 73069; e-mail: Michael.Coniglio@noaa.gov

roughly the same for 18 m s^{-1} of upper-level shear as they are for no upper-level shear and are clearly larger for intermediate shear values. It is interesting that much of the range of the observed 5-10 km shear within strong MCS environments is contained within shear values of $5\text{-}20 \text{ m s}^{-1}$ (CSR).

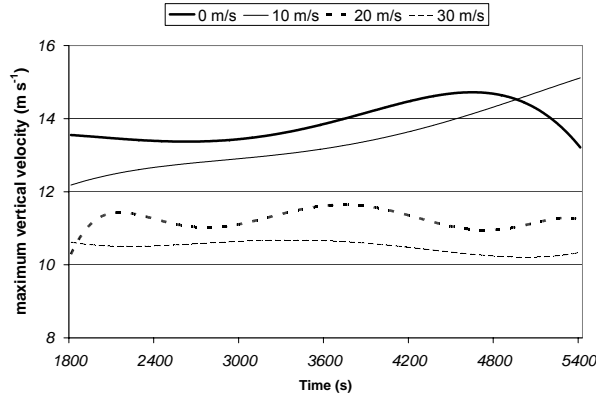


Fig. 1. Evolution of the maximum vertical velocity along the density current for the 2D simulations with 0, 10, 20, and 30 m s^{-1} of upper-level shear.

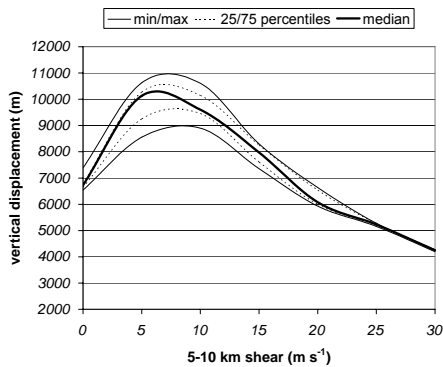


Fig. 2. The distribution of the maximum vertical displacement (m) of low-level (0-2 km) parcels for various values of 5-10 km shear. Thin solid lines enclose the maximum and minimum values among a set of 21 trajectories, thin dashed lines enclose the 25th and 75th percentiles, and the thick solid line is the median.

Insight into this basic behavior is gained through an illustration of trajectory paths for the 0 and 10 m s^{-1} shear cases (Fig. 3). For the no shear case, the parcels rise as they converge along the density current and are swept rearward relative to the gust front (Fig. 3a) forming a jump-type updraft (Moncrieff 1992). For the 10 m s^{-1} shear case, the low level parcels (0-1 km) are forced over the density current as before in a jump-type updraft (Fig. 3b). However, the parcels that begin in the 1-2 km layer overturn after they are forced upward (Fig. 3b), which results in the much larger vertical parcel displacements (Fig. 2). The flow then represents a mixed jump and overturning updraft that exists in the “steering-level” model of squall lines (Moncrieff 1992), in which the overturning is a result of a critical layer in mid levels (5-7 km). Time integration of w along the parcel

paths reveals that, despite the fact that the low level parcels experience the strongest w , the elevated parcels rise for much longer periods. With stronger upper-level shear, the perturbation high pressure (not shown) eventually limits the vertical scale of the overturning and is the reason for the decrease in maximum lifting beyond an upper-level shear of $\sim 8 \text{ m s}^{-1}$ (Fig. 2). However, this confirms the hypotheses developed in more analytical frameworks that deep-tropospheric shear with a steering level increases residence times of parcels despite lowering w along the interface. At least for the low-level shear profile and the cold pools examined in this study, the important result added by this study is that *shear added entirely above the cold pool can cause an increase in lifting associated with an overturning updraft within deep tropospheric shear* and provides a concept for how “suboptimal” systems (in the context of WR) can be enhanced in ways other than the cold pool/low-level shear interaction.

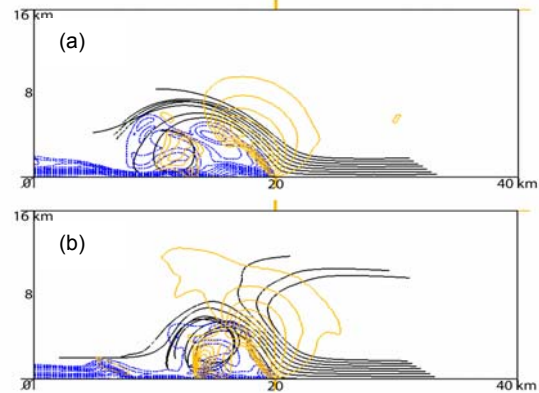


Fig. 3. Example of low-level parcel paths (thick solid lines) for the (a) 0 m s^{-1} and (b) 10 m s^{-1} upper-level shear cases. Instantaneous perturbation potential temperature (blue lines) and w (orange lines every 2 m s^{-1}) also is shown.

3. 3D RESULTS

In the 3D simulations, the prominent differences resulting from the addition of upper-level shear are found in the evolution of w and in the domain total precipitation mixing ratio (not shown). The max w for the cases with upper-level shear becomes much larger after 2 h, which coincides with the transition of the line from isolated convective cells into an organized MCS structure. Fig. 4 reveals that the case with no upper-level shear (US0 hereafter) enters an upshear-tilting phase once the cold pool becomes firmly established after 2 h. During this phase, the convective cells weaken and the precipitation becomes located farther behind the gust front, until an equilibrium state is met at $\sim 4.5 \text{ h}$. In contrast, the updrafts remain strong for the cases with upper-level shear throughout the 6 h simulation time. As in WR, these strong updrafts are partially related to the persistence of isolated supercell-like structures that develop along the outer flanks of the system. But an important distinction in this study is that the updrafts along the quasi-linear center portion of the

system are non-supercellular for the case with 15 m s^{-1} of upper-level shear (US15 hereafter) and are significantly stronger than the updrafts along the quasi-linear portion of the line in US0.

What is particularly intriguing is the role of the initial 3D structure of the cells. In US0, the cells form a solid line of heavy precipitation about 70 km in length at 2.5 h (Fig. 4a, left panel). As a result, the cold pool becomes very deep and the gust front accelerates to a speed of $> 25 \text{ m s}^{-1}$. This is accompanied by a surge in the surface wind speeds and a significant weakening of the heavy surface precipitation that becomes located farther and farther behind the gust front (Fig. 4b-d, left panels). In this scenario, all of the parcels gain an increase in rearward velocity through a faster gust front motion and stronger low-level buoyancy-pressure accelerations, as found in the 2D simulations of Parker and Johnson (2004b). In US15 however, the existence of deep-shear and 3D structure results in a line of leading convection with more gaps in the heavy precipitation initially (Fig. 4a, right panel), which leads to a shallower cold pool than what occurs in US0. With time, the precipitation solidifies along the gust front and causes it to accelerate, but to a lesser degree than what occurs in US0. Concurrently, *this surge in the gust front is not accompanied by a decrease in the surface precipitation intensity and a weakening of the updrafts in US15*. Trajectory calculations confirm that the elevated parcels are overturning in US15 by spending more time in the regions that favor upward and rear-to-front accelerations and are responsible for the strong, consolidated updrafts and the subsequent bowing in the heavy precipitation through 4 h (Fig. 4b-d, right panels). The overturning helps to maintain the more upright tilt and the strength of the convection despite the consolidation of the cells and the surge in the gust front. What facilitates the overturning is that fact that the cells maintain their 3D structures initially in US15, which leads to a reduction in the acceleration of the gust front, compared to what occurs in US0, and the maintenance of the critical layer in mid-levels. This suggests that the existence of 3D structures doesn't necessarily preclude the applicability of the 2D overturning concepts because of their effects on the cold pool depth and motion.

The increase in total rainfall with upper-level shear is partially related to the maintenance of the leading convection along the center of the line, but the primary reason is the increase in size of the systems (Fig. 5), which suggests an enhanced ability of the cold pool to initiate and maintain convection in these simulations. Along the outer flanks of the cold pool in US0, parcels are quickly swept rearward and do not convect because dry air above 3 km becomes entrained and the parcels quickly become negatively buoyant. However, in US15, the elevated parcels readily convect along the outer flanks of the slower moving cold pool because of longer residence times in the region of favorable upward accelerations and form an overturning circulation with the upward branch close to the leading edge of the gust front.

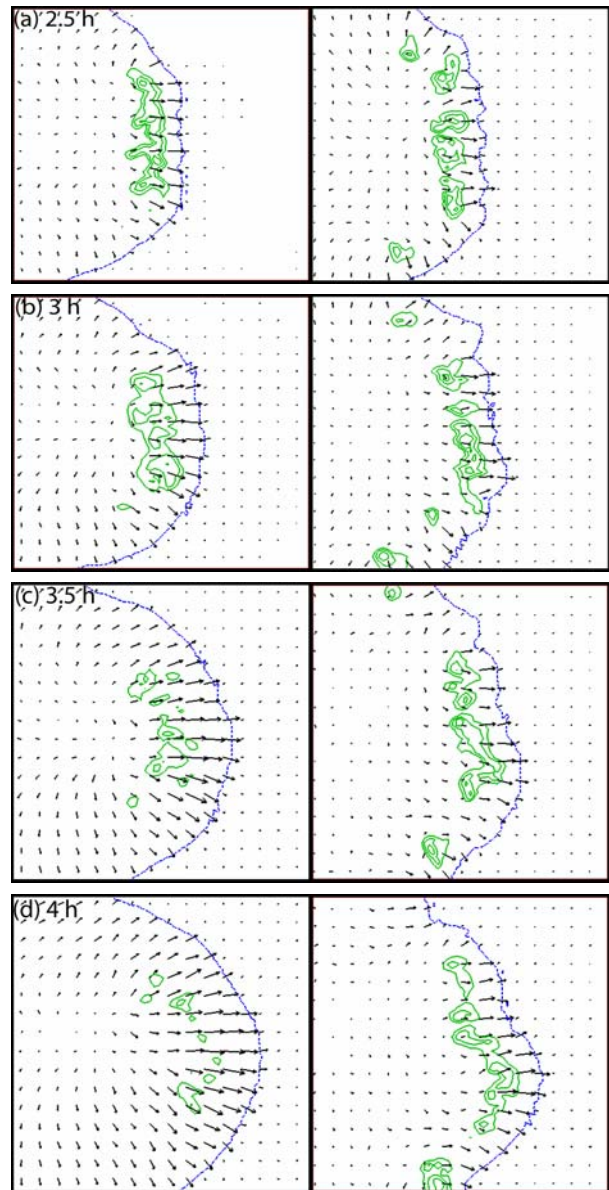


Fig. 4. Evolution of the total precipitation mixing ratio at the surface (green lines every 2 g kg^{-1}) that highlights the regions of the heaviest precipitation, the gust front (blue line) and the ground relative wind vectors (every 4 grid points) for a 120 km by 120 km portion of the domain at (a) 2.5 h, and (b) 3 h, (c) 3.5 h, and (d) 4 h for case US0 (left column) and case US15 (right column).

4. DISCUSSION

By showing that the structure and maintenance of strong MCSs is sensitive to the magnitude of the upper-level shear, we do not intend to discount the importance of the low-level shear. Although we don't know the relative sensitivities between the addition of shear in low-levels versus upper-levels, it is shown that even a modest amount of upper-level shear, added to an environment with weak to moderate low-level shear, can

have a significant impact on the structure and evolution of the simulated systems, in both quasi-2D and 3D regimes, through the variations in the depth of the overturning updraft and changes in the motion of the cold pool resulting from the 3D structure of the cells.

It should be noted that little has been said about the perceived strength of the systems. Overall, the strength of the surface winds are not very sensitive to the changes in the upper-level shear for this particular model configuration, but they are very sensitive to changes in the experimental design, particularly to the parameters in the ice-microphysics scheme. Upon changing the distribution and density of the hail species within realistic limits, the surface winds are significantly weaker in US0, but are much stronger in US15 by as much as 10 m s^{-1} in the 3-5 h time period. Although these sensitivities prevent a general assessment of how the upper-level shear affects the strength of the surface winds, the size and structure of the simulations and the tendency for the updrafts to be maintained for environments with upper-level shear is not as sensitive to these changes and provides greater confidence that the behavior of the simulations presented herein is robust.

The overturning of elevated parcels (1-2 km) may provide a concept for how strong convective systems may be maintained after the development of a surface nocturnal inversion, as long as the cold pool can be replenished, in situations without forcing from a low-level jet. However, the most applicable aspect of the overturning concept may be the prediction of the overall demise of the MCS. Indeed, observed mean storm-relative hodographs among a set of strong MCSs in weakly-forced environments show that the critical layer near 7-9 km for the beginning /mature soundings disappears for the decay soundings (Fig. 6) as a result of a significant decrease in upper-level shear. This provides observational evidence of the importance of upper-level shear and a deep overturning layer to maintaining the strength of the overall MCS.

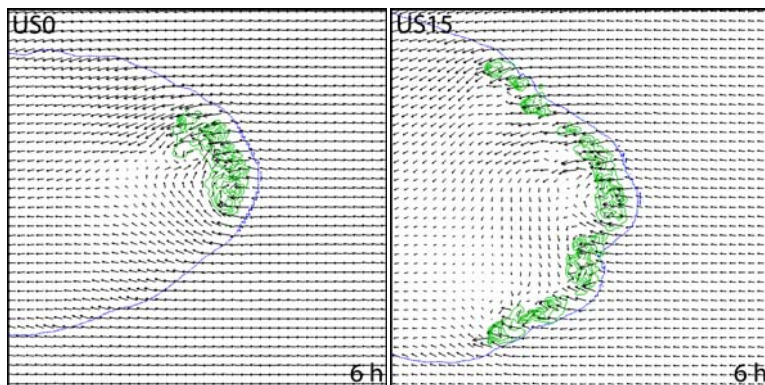


Fig. 5. Total precipitation mixing ratio at 4 km AGL (green lines contoured every 1 g kg^{-1}), the cold pool leading edge (blue line), and the storm-relative wind at 6 h for case US0 (left panel) and case US15 (right panel). A 320 km by 320 km portion of the domain is shown.

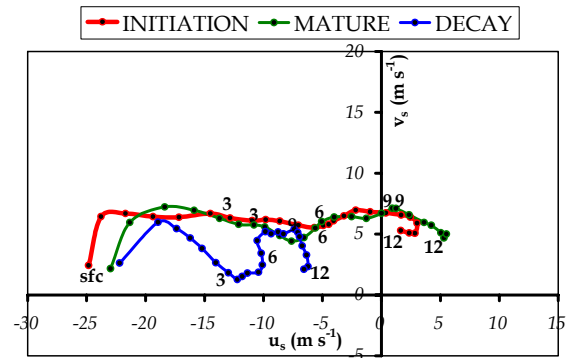


Fig. 6. Mean storm-relative hodographs for a set of 108 proximity soundings taken in the environment of strong MCSs (see CSR for a description of this data set), grouped into 29 soundings that sampled MCS initiation, 35 soundings that sampled MCS maturity, and 44 soundings that sampled MCS decay. Mean winds are calculated every 0.5 km AGL and plotted every 1 km AGL.

5. REFERENCES

- Coniglio, M.C., D.J. Stensrud, and M.B. Richman, 2004: An observational study of derecho-producing convective systems. *Wea. Forecasting*, **19**, 320-337.
- Evans, J.S., and C.A. Doswell, 2001: Examination of derecho environments using proximity soundings. *Wea. Forecasting*, **16**, 329-342.
- Moncrieff, M.W., 1992: Organized convective systems: Archetypal dynamical models, mass and momentum flux theory, and parameterization. *Quart. J. Roy. Meteor. Soc.*, **118**, 819-850.
- Parker, M.D., and R.H. Johnson, 2004a: Simulated convective lines with leading precipitation. Part I: Governing dynamics. *J. Atmos. Sci.*, **61**, 1637-1655.
- , and -----, 2004a: Simulated convective lines with leading precipitation. Part II: Evolution and maintenance. *J. Atmos. Sci.*, **61**, 1656-1673.
- Shapiro, A., 1992: A hydrodynamical model of shear flow over semi-infinite barriers with application to density currents. *J. Atmos. Sci.*, **49**, 2293-2305.
- Weisman, M.L., and R. Rotunno, 2004: "A theory for strong, long-lived squall lines" revisited. *J. Atmos. Sci.*, **61**, 361-382.
- Wicker, L.W., and Wilhelmson, R. B., 1995: Simulation and analysis of tornado development and decay within a three-dimensional supercell thunderstorm. *J. Atmos. Sci.*, **52**, 2675-2704.
- Xu, Q., and M.W. Moncrieff, 1994: Density current circulations in shear flows. *J. Atmos. Sci.*, **51**, 434-446.